Hydrodynamic model for independent cold and thermo-mineral twin springs in a stratified continental karst aquifer, Camou, Arbailles Massif, Pyrénées, France

Philippe Audra, Jean-Yves Bigot, Dimitri Laurent, Nathalie Vanara, Didier Cailhol, Gérard Cazenave

International Journal of Speleology	51 (2)	81-91	Tampa, FL (USA)	May 2022

Available online at scholarcommons.usf.edu/ijs

International Journal of Speleology

Official Journal of Union Internationale de Spéléologie

Hydrodynamic model for independent cold and thermo-mineral twin springs in a stratified continental karst aquifer, Camou, Arbailles Massif, Pyrénées, France

Philippe Audra [1*], Jean-Yves Bigot[2], Dimitri Laurent[3], Nathalie Vanara[4], Didier Cailhol[5], and Gérard Cazenave[6]

[1]Polytech'Lab EA 7498, Université Côte d'Azur, 930 route des Colles, 06903 Sophia-Antipolis, France
[2]Association française de karstologie, 21 rue des Hospices, 34090 Montpellier, France
[3]GIA Ingénierie, 114 Traverse le Mée, 13008 Marseille, France
[4]University Paris 1 – Panthéon-Sorbonne 12 Pl. du Panthéon, 75231 Paris & University Toulouse Jean Jaurès, UMR 5608 TRACES, France
[5]INRAP Toulouse, 13 rue du Négoce, 31650 Saint-Orens-de-Gameville, France
[6]Société de spéléologie et de préhistoire des Pyrénées Occidentales (SSPPO), 5 allée du Grand Tour, 64000 PAU, France

Abstract: The Camou springs (Arbailles Massif, French Western Pyrenees) display an unusual close association of a typically cold karstic spring that drains the Urgonian western limb of the Arbailles, and a thermo-mineral spring (33.5°C; salinity 17.7 g/L). The latter gains its mineralization while crossing the Triassic evaporites mainly through a deep loop in the Apanicé syncline. The fast upflow of this deep water occurs at the cross of large active lines (the North-Pyrenean thrust located at depth, and the Saison transverse fault). Cave diving in the nearby Maddalen Cave allowed reaching the phreatic passage at the origin of the cold spring, which however also crosses the thermal body in the third sump (S3). Both water bodies are separated by a sharp thermocline. Six pressure-temperature dataloggers were placed in both water bodies along the thermocline for six months. The dataloggers located downstream on either side of the thermocline show at the beginning of flood first a rise of the thermal body, then an invasion of the whole phreatic passage by the cold floodwater, controlled by head pressure changes in the karst aquifer. From observation of these mechanisms, we deduce a hydrodynamic model with a warm plume rising into the cold aquifer, without significant mixing. Such independence of water bodies is explained by the decrease of turbulent rate at the interface, due to the sharp density gradient. The relative absence of mixing does not actually require independent "watertight" routes, both water bodies can thus coexist even in the same conduit. This model locally implies the existence of unknown secondary passages close to the spring, which allow an independent draining of each water body toward separate outlets during low stage. Such type of stratified aquifer linked to density differences is common in coastal karst (Florida, French Calanques, etc.), in the continental evaporite karst (Schlotten of the Harz in Germany, Kungur karst in Ural, etc.), but remains poorly identified in continental carbonate karst areas, mainly because of the difficulty of access. Together with the Mescla Spring in French Alpes-Maritimes, the Camou twin springs discharging in the same porch are an outstanding example, allowing a direct study of the stratification and the dynamic of highly contrasted water bodies.

Keywords: hydrothermal component, various volumetric masses flows, non-mixing flows, hypogene karst, hot hydrothermal plume, cave diving

Received 10 January 2022; Revised 19 April 2022; Accepted 26 April 2022

Citation: Audra, P., Bigot, J.-Y., Laurent, D., Vanara, N., Cailhol, D., Cazenave, G., 2022. Hydrodynamic model for independent cold and thermo-mineral twin springs in a stratified continental karst aquifer, Camou, Arbailles Massif, Pyrénées, France. International Journal of Speleology, 51(2), 81-91. https://doi.org/10.5038/1827-806X.51.2.2413

INTRODUCTION

Karst springs often discharge water of various origin, in addition to the local meteoric component, but the contribution of deep flow is often hidden behind the dominant meteoric component. However, significant deep component can be suggested by the presence of particular morphologies and deposits such as travertine (Billi et al., 2016), degassing of H_2S or CO_2 (Jones et al., 2015), temperature higher than the expected values showing a thermal component (Goldscheider et al., 2010), and/or specific mineral

*Philippe.AUDRA@univ-cotedazur.fr

composition and isotopic signature (Petrini et al., 2013; Wynn et al., 2010). Along the Colorado Plateau, karst aquifers discharge abundant karst water where however one third of CO_2 load comes from deep crustal sources, including 10% of the total load originating from the mantel. Pathways for these deep fluids upflows follow active fault systems (Crossey et al., 2009). In Sierra de Tamaulipas, Mexico, in addition to meteoric water, upflow along deep-rooted fractures collects deep water enriched by volcanogenic components toward giant phreatic shafts (Gary & Sharp, 2006). In Mariovo, North Macedonia, using isotopes, Temovski et al. (2021) demonstrated that karst groundwater combines meteoric recharge with a deep hydrothermal component from crustal and mantle origin upflowing along deep faults, where it interacts with volcanic rocks, metamorphic and granitoids bodies. In Cueva de Villa Luz, Mexico, the study of this famous sulfuric cave has also shown a mixing of local shallow meteoric component with a distant recharge following deep loops gaining sulfidic and gaseous signature from sulfates and petroleum methane before upflowing (Rosales Lagarde et al., 2014; Webster et al., 2017).

In France, thermal springs in karst areas generally discharge along valleys (Lasfonts spring, Bize, Aude), sometimes even along phreatic cave passages (gourg de l'Antre, Soulatgé, Aude; Font Estramar, Salses, Pyrénées-Orientales). Some thermal caves have been explored by cave diving (Aigo Tebo, Bagnères-de-Bigorre, Hautes-Pyrénées; Mas d'En Caraman, Paziol, Pyrénées-Orientales; the phreatic shaft in Salins-les-Thermes, Savoie) (Audra, 2007). However, the close juxtaposition of springs of clearly different composition and temperature is not frequent. The Bachai di Faye, a classical cold spring discharging under the high bridge spanning over the Usses canyon is located close to the thermo-sulfuric old spa of La Caille (Allonzier-la-Caille, Haute-Savoie), however both outlets are still 300 m apart. More generally, many mineral springs occur in the vicinity of large karst water outlets, probably due to tectonically pre-disposed paths.

The presence of deep and shallow meteoric components in karst aquifers suggests several possibilities of combination, which generally evolve seasonally according to the highly variable discharge of the meteoric component. Firstly, mixing can occur at depth, thus resulting in a rather homogenous discharge of water integrating both deep and shallow inputs. Secondly, mixing can be limited with preservation of the original signature of each type of water. In this latter case, components can remain partly independent with low mixing by isolation of their respective flowpaths. Another possibility of low mixing results from the stratification of different water bodies inside the aquifer. Such occurrences are well-known in coastal karst aquifers with the classical lens of buoyant fresh water above salt water (Larson & Mylroie, 2018), in continental areas both in evaporite aquifers where meteoric seepage or surface river intrusions produces buoyant freshwater lenses onto a body of high sulfate-concentrated water (Andrejchuk, 1996), and in thermal-sourced karst aquifers (Audra & Johannet, 2021). The coastal stratified aquifers are well studied for resource protection, especially to avoid salt intrusion into freshwater aquifer. However, the continental stratified karst aquifers are generally poorly known regarding the behavior of the stratification, mainly because of limited and difficult access to the underground phreatic passages.

The Camou springs in Western Pyrenees display the double originality to discharge hot-salted and cold-fresh waters from two twin springs located in the same outlet passage, and to provide a relatively easy access to the phreatic area where a sharp thermocline separates both water bodies, which are thus clearly stratified. Some mixing can be present during given hydrologic situations; however, its dynamic suggests a behavior that allows preserving a relative independence. Consequently, Camou remains enigmatic as for its close association between a "normal" karst spring and a thermo-mineral spring. This karst aquifer, partly confined below marls necessarily displays a saturated zone of several hundreds of meters depth, certainly intensively karstified at least along some preferential areas which guide the flow (epiphreatic zone, bedding planes, and fractures). In such a context, it is difficult to figure out how thermo-mineral water can preserve its deep signature without significant mixing with cold meteoric water while crossing along fractures the whole thickness of the karstified aquifer.

It is this puzzling paradox that we studied here. After a detailed presentation of the studied springs and the investigation methods, we will display our results, which will be then discussed, to come to a conceptual hydrodynamic model that would explain this apparent paradox of "non-mixing", while eventually putting it in the general setting of the mixed aquifer with stratified bodies.

Location and description

The Camou spring (Lamiña ziloa, "the laminak Cave", the Basque springs goblins), is to our knowledge a relatively exceptional case, with two spring discharging side by side in the same porch, one hot and one cold. It is located to the south of Camou-Cihigue village (Pyrénées-Atlantiques Department), at the end of a small valley running along the eastern limb of the Arbailles massif (43.113056°N, 0.909167°W, alt. 230 m). Both springs are discharging from a short cave (Fig. 1), whereas about 10 m distance opens another portal giving access to a chamber along a fault line. About 20 m above the spring, a dig by local cavers (GS Gaves) opens to a cave system, Maddalen Cave, which connects to the underground stream at the origin of the cold spring (Fig. 2). Three successive sumps were dived, the third one (S3) has been explored down to –54 m (divers Fr. Verlaguet and D. Robert). At about 10 m depth, this S3 crosses the thermal body, which fills a low loop, whereas the upstream part of S3 is again filled with cold water. The thermal body is fed at the bottom of the loop by a narrow feeder. Both bodies are distinctly split by a sharp thermal, saline, and density transition. Such cline where density gradient is greatest within

a body of water is called pycnocline. According to its main observable physical characteristic, we will refer thereafter simply as thermocline, even if the term halocline could also be used. If the cold waters are generally clear, the thermal waters are intensively clouded by a proliferation of bacterial flakes.

Fig. 1. Inside-out view of the twin springs of Camou. At the beginning of 20th century, a low wall was built to avoid mixing between the cold spring to the left, and the hot spring to the right. A pipe led the water to the nearby farm that was set up as a medical spa (photo. J.-Y. Bigot).

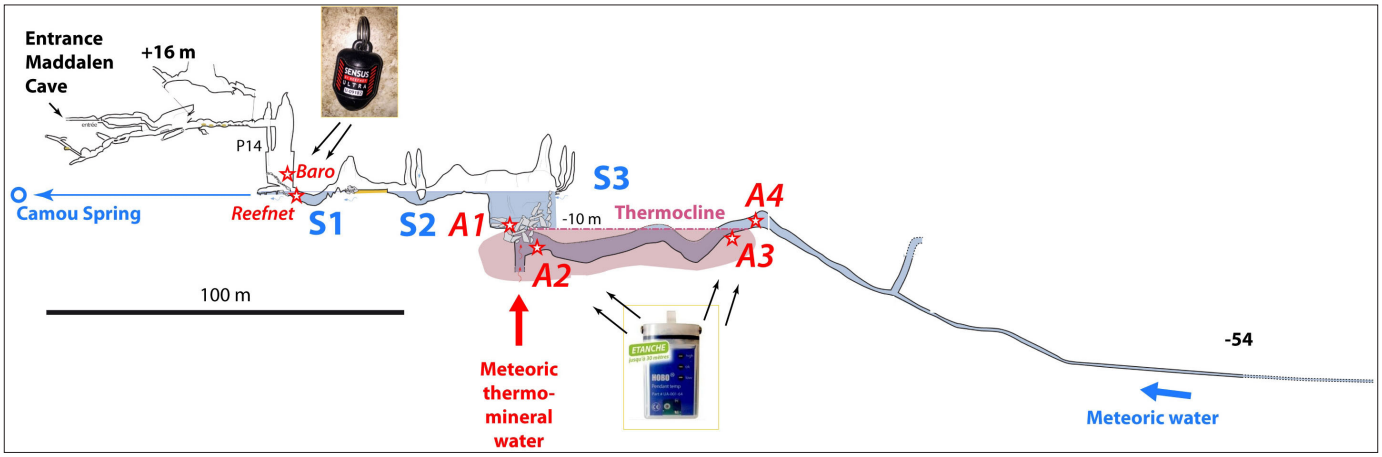

Fig. 2. Profile of Maddalen Cave (after GS Gaves, GS Oloron, Crapouillaux), with location of the dataloggers indicated by red stars (A1 to A4). S1, S2, and S3 refer to first, second, and third sumps, respectively.

Physico-chemical characteristics

Both Camou springs, although twin, are clearly distinct regarding their discharge and their physico-chemical characteristics (Fig. 3). The cold spring has a typical karstic behavior with a large variability reflecting its pluvio-nival recharge regime. Its discharge is not gauged, it can be exceptionally dry during extreme drought. Temperature varies between 14°C in high water and 27.7°C in low water, showing some mixing with the thermal component in such condition. The conductivity ranges between 2,500 and 5,000 µS/cm. Its chemical profile is typically of bicarbonate-calcium type, however with a significant portion of sulfates and chlorides, which apparently rise during high water.

As for the hot spring, it has a regular discharge of less than 1 L/s, for a temperature comprised between 28 and 38°C, and a conductivity of 19,000 – 22,000 µS/cm. It is of sodium-chloride type, with sulfates and bicarbonate-calcium. However, the total concentration (~18 g/L) is about 50 times larger than the cold spring, and the bicarbonate-calcium concentration in absolute value remains much larger than the one of the cold springs.

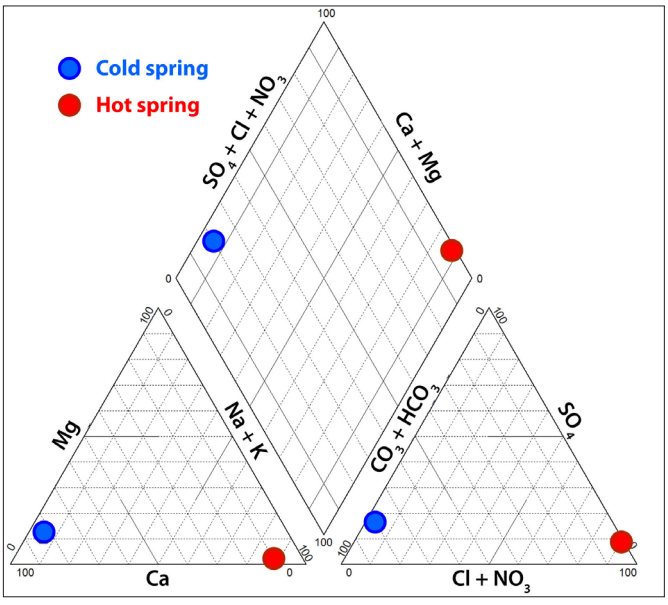

Fig. 3. Piper diagram of Camou springs, averaged from 4 samplings, each from a different season (cold spring after Inst. Européen de l'Environnement de Bordeaux, in Vanara, 2000; hot spring after Goity, 1986, in Vanara, 2000).

Hydrogeological setting

The Arbailles massif displays series of E-W folds, with the main Bidouze anticline showing a Triassic core, associated to secondary folds, bending and plunging eastward in the Apanicé marly syncline (Fig. 4). The Camou springs are located on top of the Upper Aptian limestones (Urgonian) of the anticline limb of the Arbailles massif, along an E-W fault, making an abnormal contact with the Albian black shales of the Apanicé syncline. The hydrogeologic setting shows that recharge by meteoric water logically extends to the west on the anticline limb overlooking the spring (Bechanka shaft area) and flows up across the Urgonian series when reaching the outlet.

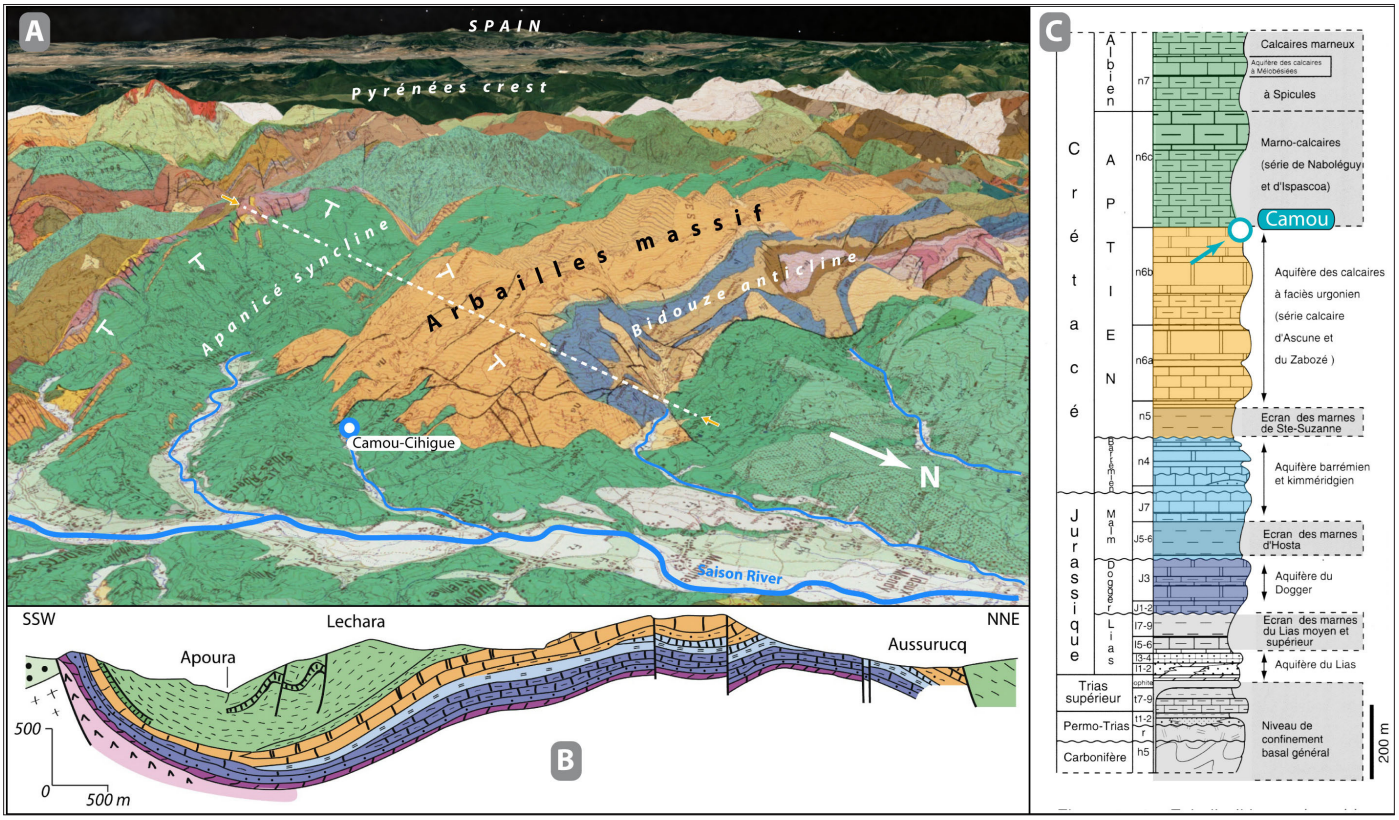

Fig. 4. Geology of the Arbailles massif. A) 3D view toward SW, with indication of the profile B and location of the Camou springs (geology from French Geological Survey. BRGM on Google Earth background). B) Geological profile (after Viaud, 1991, in Vanara, 2000). C) Stratigraphic log with location of the discharge level of the Camou springs (after Vanara, 2000).

Regarding the origin of the thermal water, the chemical facies suggest a route following a deep loop along the bottom of the Apanicé syncline, where it warms and gains the chloride-sodic and sulfate salinity at the contact with the Upper Triassic (Keuper) evaporites. This layer mainly contain gypsum, but also thick halite deposits, which are mainly present at depth (James & Canerot, 1999). Part of sulfates could also derive from solution at depth of the Jurassic limestones: the thermochemical sulfate reduction (TSR) of Triassic sulfates during Cretaceous extensional phases led to an upward migration of H_2S, that eventually has been trapped into the microporosity of these limestones (Laurent, 2019). The thermal excess of the water (+26°C), compared to the one expected at this altitude, implies a minimal depth of 900 m (for an average gradient of 1°C/33 m, in the absence of a local value), and probably more according to likely mixing and cooling along the upflow route. This upflow can be fast along the deeply rooted active regional faults. Indeed, Camou is located above the North Pyrenean Thrust Front (E-W) which crops out northward, and the Saison transverse fault (NNE-SSW) (Canerot, 2017). As for the recharge, it likely could be located along the narrow carbonate edge to the south of the Apanicé syncline, about 1,000 m asl. and 7-14 km distant. However, with such a small discharge, many other options are possible.

METHODOLOGICAL INVESTIGATIONS

Explorations of the sumps have been described, surveyed, and documented by cave divers. The dynamic of the water bodies has been recorded using autonomous waterproof dataloggers, with a sampling interval of 30 min., using Reefnet Sensus Ultra for temperature and water depth, and HOBO UA-001-64 Pendant Temp for water temperature. During six months (from 26/12/2020 to 06/08/2021), two Reefnet have been put at the downstream outlet of the first sump (S1), one immersed along the gauge scale (noted “Reefnet” on Fig. 1), the other hung above in the air for the barometric compensation (noted “Baro”). Additionally, four HOBO have been put in the first loop of S3 on either side of the thermocline, two in the downstream part, two in the upstream part (respectively noted A1 at –9 m; A2 and A3 at –11 m, A4 at –8.6 m). On the diving day, the thermocline was located at 10 m depth. All collected data were then gathered in a unique spreadsheet in order to simultaneously display the evolution curves of each datalogger. In addition, we also used data from the nearby meteorological station of Oloron-Sainte-Marie for January 2021 (Bucheli, 2021), which provided the weather conditions at a similar altitude as the Camou spring.

The video of the dataloggers setting, particularly impressive when cave divers cross the thermocline and enter into the cloudy sulfuric water, are available at the following link: youtube.com/watch?v=zHspJ9ghxuA; youtube.com/watch?v=1_w-IweYTzE.

RESULTS

During the whole 2021 period (Fig. 5), the A2 datalogger located above the thermal feeder overall remained in the thermal body, with a stable temperature of about 32°C, however, with some abrupt temperature drops resulting from the arrival of the cold water from winter floods. As for summer floods, the A2 datalogger shows thermal high-low pulses of low thermal amplitude (2 to 5°C), with some peaks reaching 37.5°C at the end of summer.

A3 and A4 dataloggers, which are located on the upstream side, remain in the cold body, around 15°C.

A1 datalogger, located downstream just above the thermocline, remains most of the time in cold water, but also shows 4 pulses of thermal water, corresponding to the flood driving force arriving after a period of moderate flow. Regarding hydrodynamic, the main flood rises (Hmax = +140 cm) correspond to the winter floods from January to March, resulting from rainfall and/or snow melting. Later floods only produce low flood rises (about +20 cm), however, well identified on the thermal signals. The shape of these thermal flood signals is very regular, with a cold pulse followed by a gradual return to the initial conditions, and on the long term with a slow trend of thermal increase. To sum up, the temperature of the cold body is at the minimum in winter, never goes below 12.5 to 13°C, and eventually slowly warms up of about 5°C on account of the gradual decrease of the cold-water input.

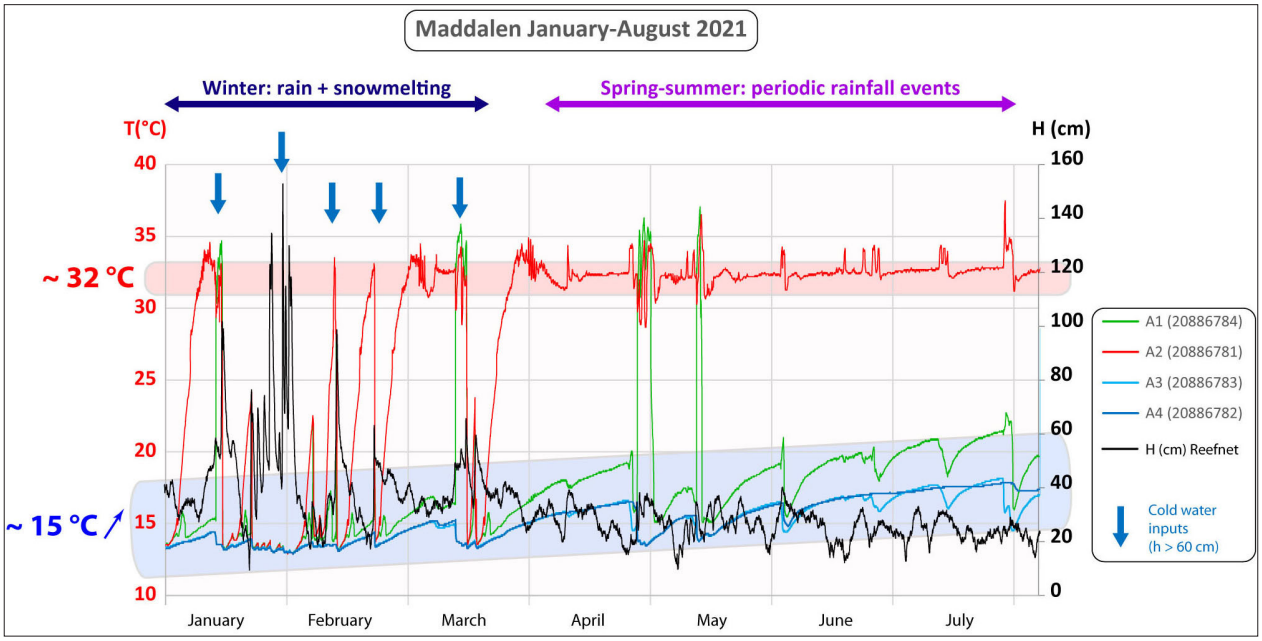

Fig. 5. Data of the thermal dataloggers deployed in the third sump (S3), from January to August 2021. Numbers to the right correspond to the dataloggers identification. Apart from abrupt flood changes, both water bodies clearly appear, a stable hot one around 32°C (datalogger A2), and a cold one around 15°C showing a gradual temperature increasing trend.

Flood signals being pretty much similar over the year with only amplitude variations, we only detail thereafter the dynamic of the January floods. The following hydrodynamic phases are noted 1 to 5 on Fig. 6:

1: In the first half of January, water level (H) is low because the low meteorological temperature stops melting of possible snow cover. Following previous large floods at the end of 2020 (H = 140 cm) when cold water invaded all passages of the S3 and homogenized the temperature, the A2 datalogger gradually returns in thermal water. Other dataloggers remained in cold water. A small thermal rise was recorded on January 5th by A1 datalogger, following a small rainfall event.

2-3: In mid-January occurs a large flood (+100 cm), associated to a return to mild meteorological conditions followed by an important rainfall on January 15th. A first moderate flood cools the upstream dataloggers (A3-A4); downstream, the thermocline rises and A1 datalogger is found in thermal water, the A2 datalogger in the thermal body is in turn slightly cooled by moderate mixing. The January 15th event provokes, in addition to a large rise of water, invasion of all dataloggers by meteoric cold water.

4: Then follows a period of mild weather without snow melting, with a gradual return to initial conditions, stopped by a return of meteoric recharge.

5: The last week of January shows oscillations (~30 cm) with a 1.5-day period that we interpret at this time as a series of snow-rain falls with immediate melting. For this period, despite the uncertainty of meteorological interpretation, successive recharge on a quasi-daily cycle is certain. This cold meteoric water input again brings to flood conditions: all dataloggers are now in cold water.

Looking more in detail to the main flood event (7 to 22 January), a hysteresis curve allows a better understanding of the hydrodynamic behavior. Temperature (T) is plotted against water depth (H),

for dataloggers A2 and A4, which are representative of the hot and the cold-water bodies, respectively. This event is characterized by the first major flood (H =100 cm) of the studied period, with significant displacement of both hot and cold-water bodies. The successive hydrodynamic phases can be described in five steps, as follows (Fig. 7):

A: 7-9 January. A recession phase occurs after a small flood during the previous days. Water depth (H) slowly decreases while A2 temperature regularly increases from 25 to 31°C, corresponding to a gradual return to steady state.

B: 9-12 January. H starts to slowly rise while A2 temperature reaches its maximum at 34.5°C. All other dataloggers, including A4, located in the cold-water body show a gentle and regular T increase. It shows that the pressure head at the origin of H increase corresponds to the arrival of floodwater very upstream in the phreatic zone that pushes forward water previously stored in the reservoir, thus slightly warmed. Both water bodies are not displaced by this moderate flood (H < 50 cm), only T of floodwater indicated the first flushing of the phreatic zone.

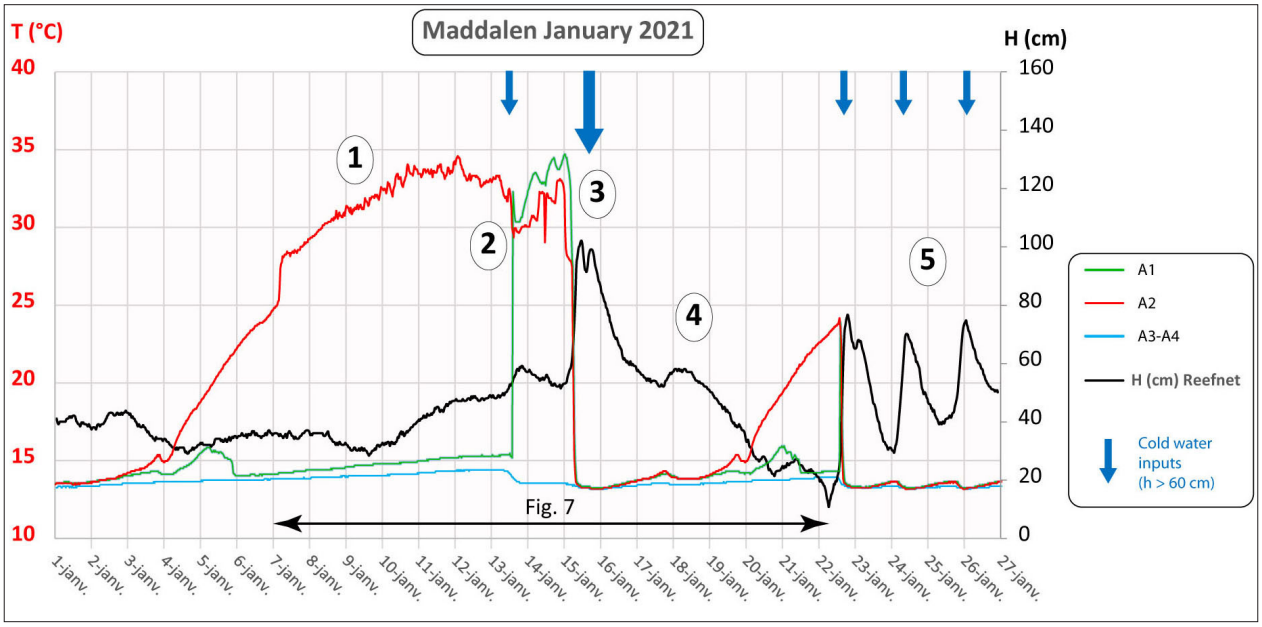

Fig. 6. Zoom on the data of thermal dataloggers settled in S3, in January 2021. A3 and A4 dataloggers having exactly the same values over this period were merged in a unique curve. Successive phases are numbered from 1 to 5 and are detailed in the text. The 7 to 22 January flood event is detailed in Fig. 7.

C: 12-13 January. Flood level continues increasing (H > 50 cm). A4 datalogger, located upstream, records the arrival of colder floodwater in the cold-water body (-1.5°C). In the hot water body (A2), some moderate mixing is shown by a slight decrease of Temperature (34.5 → 30°C). However, A1, which was located downstream, previously in cold water body just above the thermocline and 2.5 m above A2, is suddenly invaded by hot water, of same T as A2 (Fig. 6). This shows that the thermocline located between A1 and A2 is raised, due to the pressure head upstream.

D: 15 January, peak of flood (H rises to 100 cm). Temperature sharply drops to a homogeneous value (13.3°C) for all datalogger, showing a complete invasion of cold water in the whole cave system.

E: 15-22 January, recession. H drops to its lowermost level (10 cm); Temperature of A2 starts rising fast when H < 30 cm, whereas A4 returns to its initial temperature (14°C). Both hot and cold-water bodies tend to return to the initial "isolated" conditions, with minimal thermal mixing.

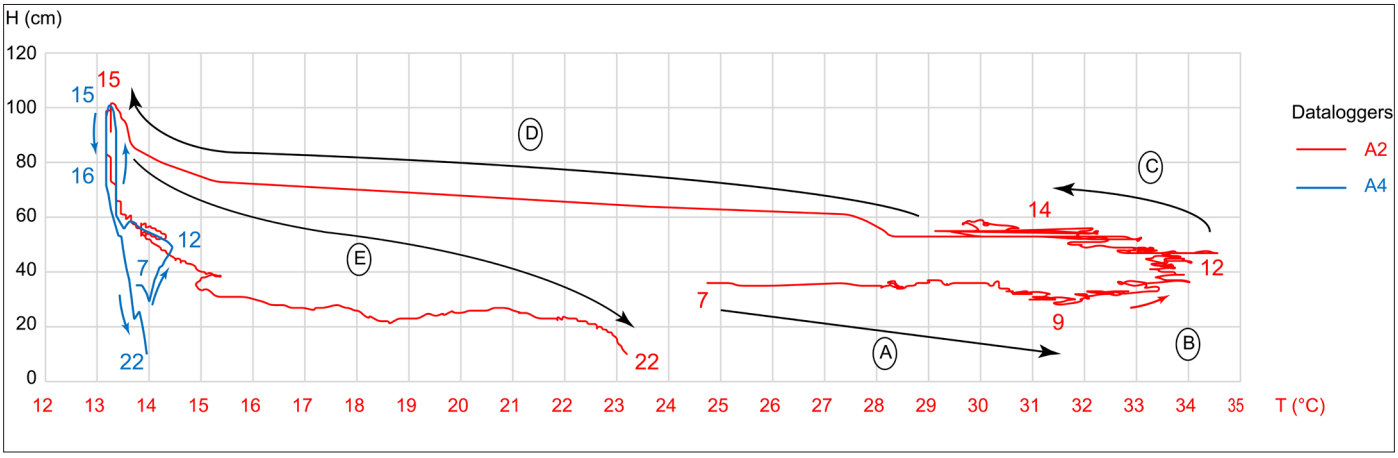

Fig. 7. Hysteresis curve of the 7 to 22 January flood event (corresponding days are indicated along the curves by numbers), where temperature (T) is plotted against water depth (H). Dataloggers A2 and A4 are located in hot and cold water, respectively, during steady state. Successive phases are numbered from A to E and are detailed in the text.

The thermal and water depth data of the dataloggers allow understanding the hydrodynamic during a flood phase, that comes out as a vertical displacement of the thermocline (Fig. 8). The thermal water, even warmer, is denser because of its salinity: thus, the cold meteoric water body remains above, whatever the flow conditions. During low water (Fig. 8A), both water bodies are in steady state, and only A2 datalogger is in hot water. The upstream A3 datalogger, even if located at the same depth as A2 (the cave divers depth gauges are precise) is for this stage in cold water. This inclination of the thermocline is interpreted as resulting from upstream meteoric water input, making a subtle pressure difference on the thermal body. The draining of the cold-water body does not happen through the phreatic passage, whose low loop remains filled with thermal water, without any sign of significant mixing.

At the beginning of flood (Fig. 8B), the growing input of cold meteoric water increases the pressure head on the upstream side of the sump. In this transitory stage, the hot stagnant water located in the S3 loop is pushed downward by cold water arriving from upstream, by piston-flow effect, then A1 datalogger is also in hot water. Finally, at the maximum flood, the pressure head of the cold-water body is high enough to block the thermal water into the feeder; all the low loop is invaded by the cold water that flows in abundance toward the spring (Fig. 8C).

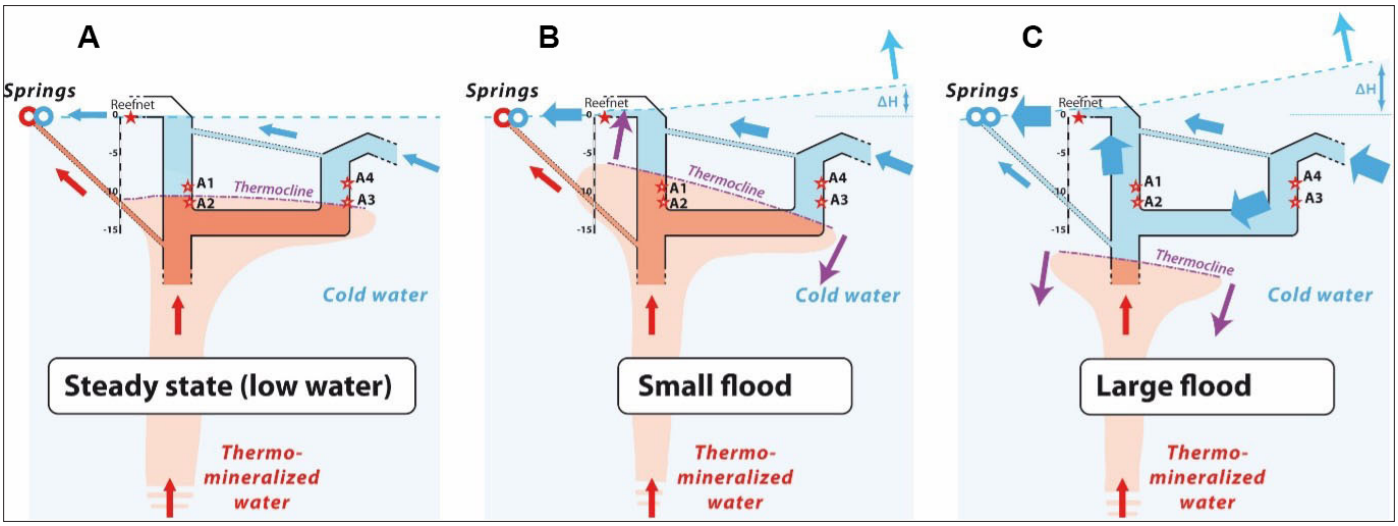

Fig. 8. Hydrodynamic interpretation model of the behavior of the water bodies stratification in S3 depending on hydrologic conditions. See text for explanation.

DISCUSSION

Differential density

The very clear thermocline shows the presence of two water bodies with clearly different physical characteristics, and which do not significantly mix. However, such interface only results in a subtle density difference: 1,006 kg/m^3 for the thermal body (with T = 35°C and salinity = 17.5 g/L), and 999 kg/m^3 for the meteoric water (with T = 15°C and salinity = 0.4 g/L). This corresponds to a difference of 0.72% that is only 1/138, whereas the "classical" gap between freshwater and saline seawater is 1/40.

Hydrodynamic model of low-mixing flow

If two different water masses are stationary, they will mix at a rate provided by thermal and mass diffusion. If the mass diffusivity is smaller than the heat diffusivity, then the temperature will even out in the mixing layer faster than the salinity. Diffusion mixing is a very slow process. The thickness of the mixing layer is given by a relationship of the form $L = \sqrt{(Dt)}$, where D is the diffusivity, and t is the observation time.

The value of the two diffusivities D at 25°C is $1.6 \cdot 10^{-9}$ m^2/s for NaCl and $1.43 \cdot 10^{-7}$ m^2/s for heat (Rumble et al., 2021, p. 576), i.e., a ratio between the two of 90. The ratio of penetration lengths will therefore, for comparable times, be of the order of nine. Heat will therefore diffuse much more easily than salinity. This means that at the thermocline, the density difference will tend to increase rather than decrease, thus hindering mixing. It is effectively admitted, in the frame of flows with various volumetric masses, that the rate of turbulent mixing in stratified fluids significantly decrease close to the interface (Viollet, 2001). However, when the two waters are in motion, the turbulence of the mixing layer is attenuated (Viollet, 2001), and in this case the mixing will be much faster.

This hydrodynamic behavior implies the presence of unknown passages, likely as narrow conduit or fissures, which allow the parallel draining of both water bodies toward distinct outlets. On the model, we hypothetically represented the thermal drainage fissure on top of the feeder and the flood interface below, which is only one possibility (Fig. 8).

During low water, the stratification is in steady state, the draining occurs through those unknown fissures feeding two springs having highly contrasted characteristics. Such a setting allows the independence of both flows, without significant mixing. During high water, the pressure head increase in the meteoric body produces a subsidence of the thermocline interface, so that the thermal water is blocked into the feeder. The cold water then uses any passages, and therefore both springs become cold. In both situations, low water and flood,

one can consider that mixing is very limited, even when a conduit is occupied by two differentiated water bodies.

Analogy with saline contamination in large coastal aquifers

Our model of plume upflow, moved by a forced convection due to the pressure of the dense hydrothermal flux upflowing in a less dense meteoric aquifer, is relatively similar to the dynamic of a multilayer aquifer such as the Florida one, with only scaling difference (Fig. 9). In Florida, the deep saltwater flows up as brackish plumes across the multilayer freshwater aquifers, crossing the confining units along fractures (Spechler, 1994; Klimchouk, 2017). Such thermal- and salinity-induced convection already existed before, however being dramatically forced by water pumping that put a strain on the whole aquifer, inducing salt contamination of the freshwater aquifers.

Such a setting is common, if not systematic, in coastal karsts. The meteoric water is drained toward the sea, whereas the sea saltwater penetrates into the continental aquifer, especially along the karst conduits (Arfib, 2001; Ginés & Ginés, 2007; López-Martínez et al., 2014). The salt wedge, well-known by cave divers, perfectly shows this stratification of low-mixing bodies, where the buoyant meteoric light water occupies the highest part of the conduits and "floats" above the salt wedge. The latter can penetrate along the floor of conduits over pluri-kilometric distances. The Port-Miou example, in the Calanques of Marseille, is one of the most famous.

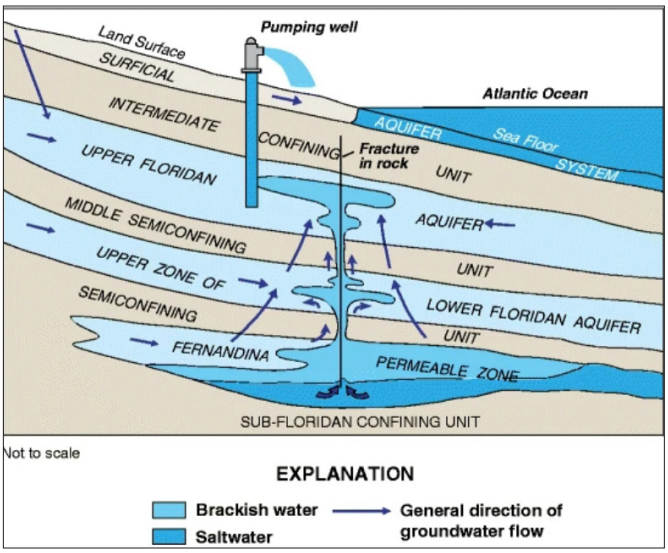

Fig. 9. Hydrodynamic model of the Florida multilayer aquifer, with stratified water bodies and upwelling of dense brackish waters due to increased pumping (Barlow, 2016).

Other contexts of karst aquifer stratifications

The stratification of water bodies also occurs in phreatic cave system developed in evaporites. Fresh meteoric water, coming either from seepage or nearby surface river intrusion, "floats" as lenses over a high-concentrated saline water, which is saturated after a long residence time. This is the case of Orda Cave, developed in gypsum, along the Kungur River in Ural (Andreychouk, 1996). At greater depth, such water stratifications have been evidenced by mining pumping in the anhydrite of the Harz Massif, Germany. Here, the sulfate rock is dissolved by unsaturated upflows coming from the underlying carbonate aquifer. It results in huge cave systems, the Schlotten, which are deep-phreatic hypogene caves (Fig. 10). Deep feeders provide fresh water at the origin of stratification, illustrated by notches developed at the interface between both water bodies and by the development of solution facets (Fazetten) below (Kempe et al., 1975).

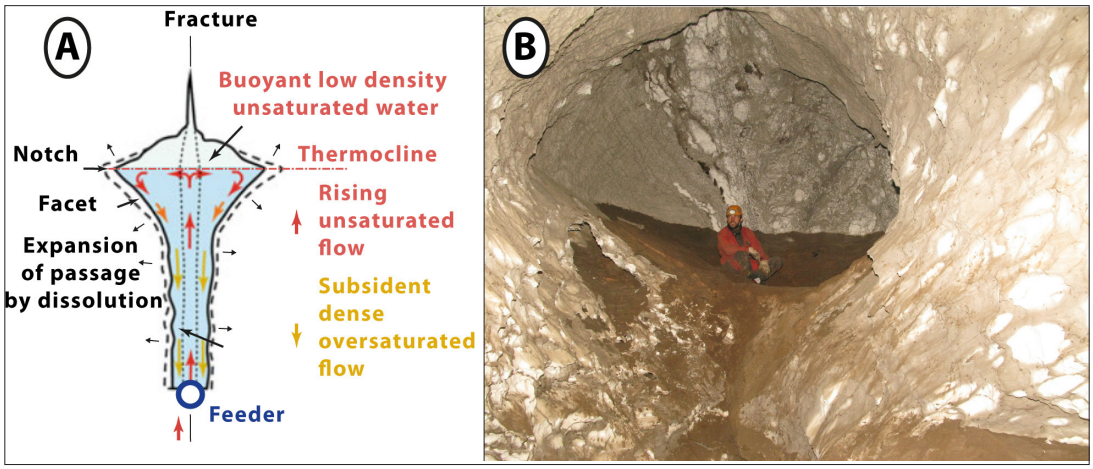

Fig. 10. A) Model of recharge of deep hypogene passages in evaporites, with stratification of water bodies of various density and development of notches along the interface (after Klimchouk & Andreychouk, 2017). B) Notch and convective facets in anhydrite, Elisabeth Schlotten, Harz Massif, Germany (photo M. Brust).

Finally, in continental carbonate karsts, the observation of a similar situation is rare and seems to be limited to the aquifers comprising thermo-mineral components. In any case, it has not been often demonstrated, probably due to the difficulties of access and observation of such deep phreatic karsts. In the Mescla Cave, Alpes-Maritimes, France, the main aquifer body consists of saline and thermal water corresponding to the deep component, over which "float" freshwater lenses fed by meteoric infiltration through the vadose zone (Fig. 11, Audra & Johannet, 2021). Such a configuration requires: (i) the presence of evaporites at depth responsible for the increase of saline concentration and stratification, and (ii) hydrothermal fluxes allowing the upflow of the deep waters. The Mescla case is rather similar to Camou, however having its hydrothermal component located far upstream, whether it is located close to the outlet at Camou.

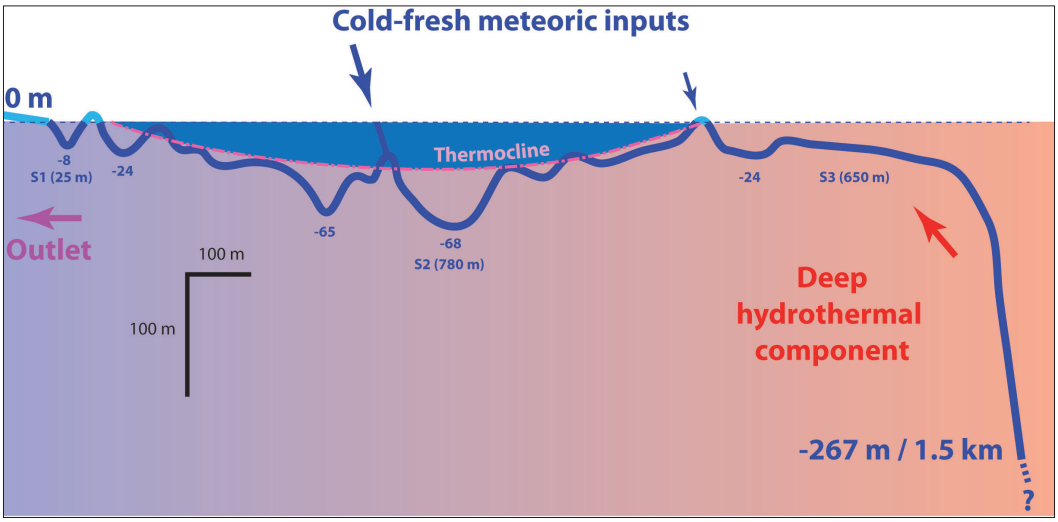

Fig. 11. Water bodies stratification in a thermal-saline aquifer, Mescla Cave, Alpes-Maritimes, France (Audra & Johannet, 2021). S1, S2, and S3 refer to first, second, and third sumps, respectively. Note that horizontal and vertical scales are different.

CONCLUSION

With this study of the Camou twin springs, a cold-fresh and a brackish-hot one, in the Arbailles massif, Pyrenees, we suggest a hydrodynamic model explaining the paradoxical juxtaposition of these two springs showing so different physico-chemical characteristics. No need to evoke any totally independent and "watertight" routes, which are not compatible at all with the concept of intensively karstified aquifers. Thanks to dataloggers placed by cave divers in the main conduit on either side of the thermocline, we show that the physical differences between both water bodies, the deep saline and the fresh meteoric, are enough to limit mixing, even when both water bodies neighbor into the same conduit. In that case, the thermocline can persist despite very limited density differences, due to the high salinity contrast decreasing the turbulent mixing rate close to the interface. Such stratification is in steady state during low water, where each water body drains toward its own spring using small conduits or fissures. In a transitory way, floods modify this equilibrium by producing a pressure head upstream in the meteoric aquifer, which pushes downwards the thermocline, temporarily blocks the upflow of the thermo-mineral flux, and discharges cold water to both springs. Such stratified setting, well-known in coastal and evaporite aquifers, however, is poorly described in continental carbonate aquifers, mainly because of the difficulties of observation in these deep phreatic karsts. Such stratification requires (i) the presence of saline layers at depth; (ii) hydrothermal fluxes allowing the upflow of the deep thermo-saline waters, which acquired their characteristics at depth. These plumes of thermo-mineral waters can neighbor within the fresh-cold water in the aquifer, the mixing of so different water bodies being finally very limited at least in steady state, and (iii) both parts of the stratified aquifer are driven by differently changing pressure mechanisms, including the thermal one which is likely not totally constant. The recharging pressure front of the cold-water component has the determining position on the whole system.

For future development, in addition to the current dataloggers, continuous monitoring (H, T, and EC) of both cold-fresh and warm-salted springs would enable a better understanding to the processes only briefly described here. Regardless, Camou spring remains an outstanding case study, with the rare possibility of direct access and monitoring of the water bodies stratification and the dynamics of the thermocline, which is controlled by seasonal recharge. Our results can shed light and attract more interest to similar cases, which however remain poorly identified although with seldom appearance, cases.

ACKNOWLEDGEMENTS

We are infinitely grateful to cave divers for their warm and friendly help for dropping and taking back the dataloggers: Frédo Verlaguet, Émilie Perret, Rémi Bertrand, Ludovic Bailly. We also acknowledge Jean-Baptiste Aguer, for permission of diving in his property, Brice Maestracci and Frédo Verlaguet for pictures, Baudouin Lismonde and Bruno Arfib for the scientific discussions and comments of the draft. We are also particularly grateful to the three anonymous reviewers and to the editor for their helpful comments and suggestions.

Authorship statement: NV, DC, DL, and GC participated to the field work. JYB managed field work and helped designing the model. PA designed and directed the study, proceeded the data, and wrote the paper with input from all authors.

REFERENCES

Andrejchuk, V., 1996. Gypsum karst of the pre-Ural region, Russia. International Journal of Speleology, 25(3-4), 285–292. http://dx.doi.org/10.5038/1827-806X.25.3.22

Arfib, B., 2001. Study of groundwater flows in coastal karstic aquifer: observations and modeling of the brackish spring Almyros of Heraklio, Crete (Greece) (in French). Thesis, University Pierre et Marie Curie, Paris, 343 p.

Audra, P., 2007. Epigene and hypogene karst and speleogenesis. Operative research and valorisation (in French). Habilitation Thesis, University of Nice Sophia Antipolis, 278 p. http://dx.doi.org/10.13140/RG.2.2.27333.27360

Audra, P., Johannet, A., 2021. Monitoring of Mescla karst spring in the French Southern Alps. A rare case of stratified waters out of coastal area. 28th International Karstological School "Classical karst", Regional karstology – Local and general aspects, June 2021, Postojna, Slovenia. https://doi.org/10.13140/RG.2.2.14944.40965

Barlow, P.M., 2016. Ground water in freshwater-saltwater environments of the Atlantic Coast. USGS Circular, 1262, 113 p. https://pubs.usgs.gov/circ/2003/circ1262

Billi, A., De Filippis, L., Poncia, P.P., Sella, P., Faccenna, C., 2016. Hidden sinkholes and karst cavities in the travertine plateau of a highly-populated geothermal seismic territory (Tivoli, central Italy), Geomorphology, 255, 63–80. https://doi.org/10.1016/j.geomorph.2015.12.011

Bucheli, B., 2021. Meteo Amikuze, Station Oloron-Sainte-Marie, http://www.oloron-ste-marie.meteoamikuze.com/Statistiques.html (accessed: Dec., 2021)

Canérot, J., 2017. The pull apart-type Tardets-Mauléon Basin, a key to understand the formation of the Pyrenees. BSGF - Earth Sciences Bulletin, 188(35), 14 p. https://doi.org/10.1051/bsgf/2017198

Crossey, L.J., Karlstrom, K.E., Springer, A.E., Newell, D., Hilton, D.R., Fischer, T., 2009. Degassing of mantle-derived CO_2 and He from springs in the southern Colorado Plateau - Neotectonic connections and implications for groundwater systems. Geological Society of America Bulletin, 121(7-8), 1034–1053. https://doi.org/10.1130/B26394.1

Gary, M.O., Sharp, J.M. Jr., 2006. Volcanogenic karstification of Sistema Zacatón, Mexico. In: Harmon, R.S., Wicks, C.M. (Eds.), Perspectives on karst geomorphology, hydrology, and geochemistry - A tribute volume to Derek C. Ford and William B. White, GSA Special Paper, 404, 79–89. https://doi.org/10.1130/2006.2404(08)

Ginés, A., Ginés, J., 2007. Eogenetic karst, glacioeustatic cave pools and anchialine environments on Mallorca Island: a discussion of coastal speleogenesis. International Journal of Speleology, 36(2), 57–67. https://digitalcommons.usf.edu/ijs/vol 36/iss2/1

Goldscheider, N., Mádl-Szőnyi, J., Erőss, A., Schill, E., 2010. Thermal water resources in carbonate rock aquifers. Hydrogeology Journal, 18, 1303–1318. https://doi.org/10.1007/s10040-010-0611-3

James, V., Canerot, J., 1999. Diapirisme et structuration post-triasique des Pyrénées occidentale et de l'Aquitaine méridionale (France). Eclogae Geologicae Helvetiae, 92(1), 63–72. http://doi.org/10.5169/seals-168647

Jones, D.S., Polerecky, L., Galdenzi, S., Dempsey B.A., Macalady J.L., 2015. Fate of sulfide in the Frasassi cave system and implications for sulfuric acid speleogenesis, Chemical Geology, 410, 21–27. https://doi.org/10.1016/j.chemgeo.2015.06.002

Kempe, S., Brandt, A., Seeger, M., Vladi, F., 1975. "Facetten" and "Laugdecken", the typical morphological elements of caves developing in standing water. Annales de Spéléologie, 30(4), 705–708. https://www.researchgate.net/publication/233925332

Klimchouk, A., 2017. Types and settings of hypogene karst. In: Klimchouk, A., Palmer, A.N., De Waele, J., Auler, A., Audra, P. (Eds.). Hypogene karst regions and caves of the world. Cave and karst systems of the world. Springer, Cham, 1–39. https://doi.org/10.1007/978-3-319-53348-3_1

Klimchouk, A., Andreychouk, V., 2017. Gypsum karst in the southwest outskirts of the Eastern European Platform (Western Ukraine): A type region of artesian transverse speleogenesis. In: Klimchouk A., Palmer A.N., De Waele J., S. Auler A., Audra P. (Eds.), Hypogene karst regions and caves of the world. Springer, Cham, p. 363–385. https://doi.org/10.1007/978-3-319-53348-3_23

Larson, E.B., Mylroie, J.E., 2018. Diffuse versus conduit flow in coastal karst aquifers: the consequences of island area and perimeter relationships. Geosciences, 8(7), 268. https://doi.org/10.3390/geosciences8070268

Laurent, D., 2019. A sulfuric acid speleogenesis in the northern Pyrenees? Example of the Arbailles karstic region (West Pyrenees, France). EGU General Assembly 2019, Geophysical Research Abstracts, vol. 21. https://meetingorganizer.copernicus.org/EGU2019/EGU2019-10137.pdf

López-Martínez, R., Gázquez, F., Calaforra, J.M., Audra, P., Bigot, J.Y., Pi Puig, T., Alcántara-Hernández, R.J., Navarro, A., Crochet P., Corona Martínez, L., Daza Brunet, R., 2020. Bubble trail and folia in cenote Zapote, Mexico: petrographic evidence for abiotic precipitation driven by CO_2 degassing below the water table. International Journal of Speleology, 49(3), 173–186. https://digitalcommons.usf.edu/ijs/vol49/iss3/1

Petrini, R., Italiano, F., Ponton, M., Slejko, F.F., Aviani, U., Zini, L., 2013. Geochemistry and isotope geochemistry of the Monfalcone thermal waters (northern Italy): inference on the deep geothermal reservoir. Hydrogeology Journal, 21, 1275–1287. https://doi.org/10.1007/s10040-013-1007-y

Rosales Lagarde, L., Boston, P.J., Campbell, A.R., Hose, L.D., Axen, G., Stafford, K.W., 2014. Hydrogeology of northern Sierra de Chiapas, Mexico: a conceptual model based on a geochemical characterization of sulfide-rich karst brackish springs. Hydrogeology Journal, 22(6), 1447–1467. https://doi.org/10.1007/s10040-014-1135-z

Rumble, J.R. Jr. (Ed.), 2021. Ionic conductivity and diffusion at infinite dilution. CRC handbook of chemistry and physics (102th Ed.), CRC Press/Taylor & Francis, Boca Raton, 1604 p.

Spechler, R.M. 1994. Saltwater intrusion and quality of water in the Floridan Aquifer System, Northeastern Florida. Water-Resources Investigations Report, 92-4174, USGS, 76 p. https://doi.org/10.3133/wri924174

Temovski, M., Túri, M., Futó, I., Braun, M., Molnár, M., Palcsu, L., 2021. Multi-method geochemical characterization of groundwater from a hypogene karst system. Hydrogeology Journal, 29, 1129–1152. https://doi.org/10.1007/s10040-020-02293-w

Vanara, N., 2000. The Arbailles karst (in French). Karstologia Mémoires, 8, Thesis, Université. Bordeaux 3, 320 p.

Viollet, P.-L., 2001. Mechanics of fluids with varying volumetric mass. Aerodynamics, thermodynamics, stratified flows, heat transfers (in French). Presses de l'École nationale des Ponts et Chaussées, Paris, 244 p.

Webster, K.D., Rosales Lagarde, L., Sauer, P.E., Schimmelmann, A., Lennon, J.T., Boston, P.J., 2017. Isotopic evidence for the migration of thermogenic

methane into a sulfidic cave, Cueva de Villa Luz, Tabasco, Mexico. Journal of Cave and Karst Studies, 79(1), 24–34. https://doi.org/10.4311/2016es0125

Wynn, J.G., Sumrall, B., Onac, B.P., 2010. Sulfur isotopic composition and the source of dissolved sulfur species in thermo-mineral springs of the Cerna Valley, Romania. Chemical Geology, 271, 1-2, 31–43. https://doi.org/10.1016/j.chemgeo.2009.12.009